BREAKUP MAGMATISM ALONG THE ARGENTINA CONTINENTAL MARGIN

Patricio Figueredo[1], Garry Karner[2], Russell Mapes[1], Kyla Simons[1]

1: ExxonMobil Upstream Company, Global New Opportunities. patricio.h.figueredo@exxonmobil.com

2: ExxonMobil Technology and Engineering Company, Structure and Hydrocarbon Systems Modeling

Keywords: crustal framework, seaward-dipping reflectors, abandoned spreading center

RESUMEN

El segmento del margen del Atlántico Sur al sur de la Cadena Florianópolis-Walvis exhibe ejemplos excelentes de la interacción de procesos tectónicos y magmáticos durante la ruptura litosférica. En este contexto, la presencia de paquetes conjugados de reflectores buzantes hacia el mar (*seaward-dipping reflectors*, SDR) provee importante información acerca de la paleogeografía, la historia de relleno sedimentario de los depocentros tempranos, y la datación del momento de ruptura. En este trabajo, repasamos la información extraída a partir de la interpretación de morfología de los SDR, deltas de lava, y la migración de dorsales en el margen continental argentino y su opuesto, los cuales parecen reflejar un largo período de restricción y aislamiento de la cuenca previo a la incursión marina en el Aptiano, favoreciendo así la posibilidad de acumulación de reservorios y sedimentos ricos en materia orgánica.

Hemos integrado interpretaciones tectono-estratigráficas de datos sísmicos 2D de la cuenca Argentina profunda recientemente adquiridos por TGS, anomalías magnéticas y gravimétricas, y observaciones del margen conjugado sudafricano en un modelo consistente de la evolución tectónica y paleogeográfica de la región. Las direcciones de corteza oceánica más reciente, combinadas con extrapolaciones de anomalías magnéticas, nos han permitido identificar las piezas de corteza oceánica en el área de estudio que fueron capturadas del margen sudafricano por dorsales abandonadas en el Cretácico Temprano. Adicionalmente, como la edad de ruptura y el momento y vector, de NO-SE a E-O, del cambio de dirección de apertura en el área de estudio parecen ser similares a los de las cuencas de Santos y Campos, es posible que la dirección de transporte tectónico de todo el margen Sudamericano pre-M4 haya sido el mismo que la de las dorsales desorganizadas que identificamos en la cuenca Argentina. Es más, podemos especular que un modelo de ruptura sincrónica, a diferencia de ruptura progresiva hacia el norte, es viable para todo el Atlántico Sur austral.

ABSTRACT

The segment of the South Atlantic margin south of the Florianopolis-Walvis ridge exhibits excellent examples of the interaction of tectonic and magmatic processes during lithospheric breakup. In this context, the presence of conjugate sets of seaward dipping reflectors (SDR) provides important information on the paleogeography, the sediment infill history of the early depocenters, and the timing of breakup. In this contribution, we review the insights extracted from the interpretation of SDR morphologies, lava deltas, and spreading center migrations on the Argentina continental margin and its conjugates, all of which seem to indicate a substantial period of basin isolation and restriction prior to the main marine incursion in the Aptian, thereby leading to the possibility for deposition of organic-rich sediments and reservoirs.

We have integrated tectono-stratigraphic interpretations of recently acquired TGS Argentina Deepwater Basin 2D seismic data, magnetic and gravity anomalies, and observations from the conjugate margin in South Africa into a consistent tectonic and paleogeographic evolution model for the region. Younging directions, as seen in oceanic crustal fabrics, combined with extrapolations of magnetic chrons, enabled us to identify pieces of oceanic crust in the study area that were captured from the African margin by a series of ridge jumps in the Early Cretaceous. In addition, as breakup age and the change in spreading direction and timing from NW-SE to E-W for the area of study appear to be similar to that of the Santos and Campos basins, it is thus possible that the entire pre-M4 tectonic transport direction along the southern South American margin had the same orientation as the disorganized spreading centers mapped in the Argentina Basin. Further, we speculate that synchronous breakup, rather than northward unzipping, is a viable model for the entire southern South Atlantic.

1. Introduction

The earliest record for the formation of the southern Atlantic lies in the deep waters of Argentina and Uruguay and their African conjugates. Previous workers have interpreted a relatively simple, dominantly orthogonal, initial opening of the basin and a smooth transition from rift to drift (Kress *et al.* 2021; Lovecchio *et al.* 2020). However, integration of newly available 2D seismic (TGS-Spectrum) and high-resolution gravity data (Sandwell *et al.* 2013) suggest a more complex history. Detailed interpretation of basin opening has historically been biased with data collected from the African margin because industry activity on the outer shelf and slope of southeastern South America developed more slowly. Early offshore exploration of Argentina occurred exclusively on the wide continental shelf, and the few wells that were drilled unsuccessfully targeted continental, lacustrine, and shallow marine deposits that gave little context on how and when the deep-water basin opened. To date, no deep-water wells have been drilled that penetrate deeper than the early Cenozoic, so all descriptions of Cretaceous lithology and timing remain interpretive and uncertain. Similarly, it was not until the 2000s that modern 2D seismic surveys were acquired over the continental slope and into the deep-water, and not until the late 2010s that sufficiently dense 2D seismic grids existed, to provide subsurface images with which to interpret complexities of the basin history (Figure 1). In this contribution, we present an interpretive framework for describing early basin history and a new integrated view of events that occurred during opening of the southern South Atlantic based on heritage and new data available on the South American and African margins.

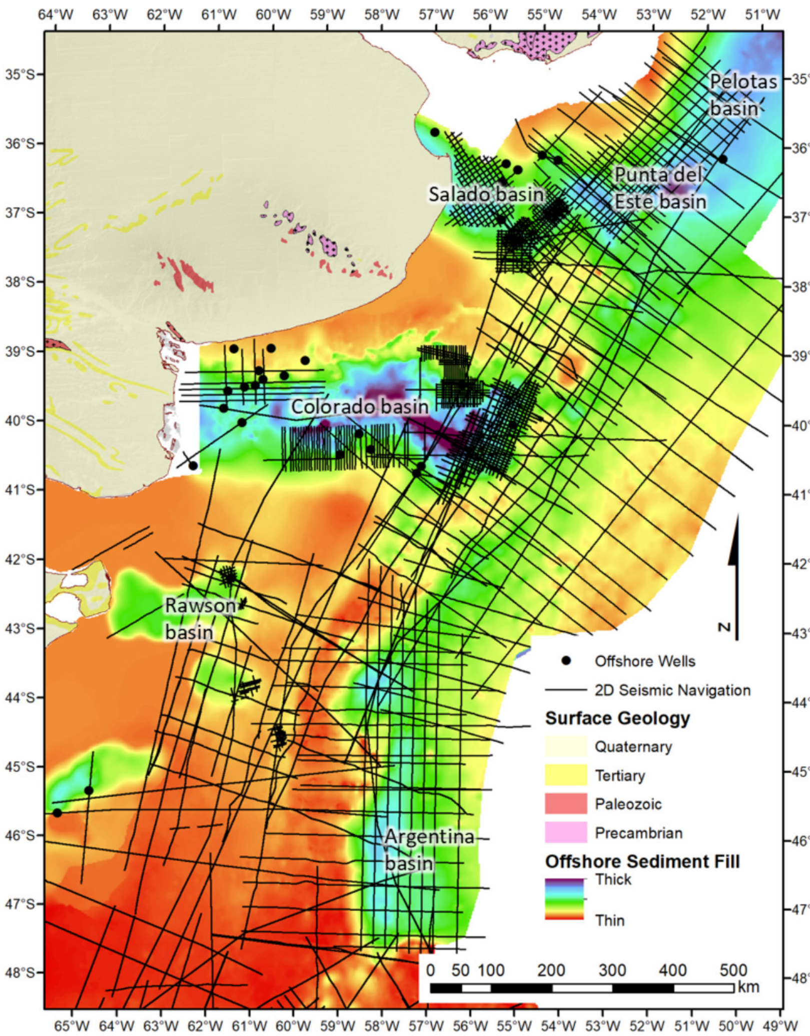

Figure 1. Argentina and Uruguay offshore seismic and well database. Geologic map shown for onshore areas (Goudarzi 1977). Total sediment thickness displayed for offshore areas.

In this contribution, we review the age of breakup along the South American margin, from southern Argentina to the Santos basin, and relook at the question of margin diachroneity from south to north, at least for the southern South Atlantic. The question becomes, how much of this SDR crust represents disorganized seafloor spreading whose convoluted magnetic signature cannot be easily recognized as a correlatable seafloor spreading anomaly? We further investigate the development of the southernmost Argentine oceanic crust to determine its age, environments of deposition, and links to conjugate crust offshore South Africa. We present an interpretive framework for the early basin history of the margin and a new integrated view of events that occurred during the early opening of the southern South Atlantic based on heritage and new data available on the South American and West African margins.

2.1. Determining crustal types

To determine crustal types, we combine crustal thickness estimates with key seismic observations, which are summarized in a series of sketches shown in Figure 2. Following the observations and discussion presented elsewhere (Figueredo *et al.* 2017; Karner *et al.* 2021), here we delineate the seismic criteria we developed to map and interpret crustal domains associated with breakup and magmatism, reflecting a gradual transition from tectonic to magmatic processes. Note that not all the described crustal types are present in the Argentina-Uruguay margin study area.

Thinned continental crust is the consequence of extension of the upper crust by low-angle normal faults that tend to detach at mid-crustal levels, while the lower crust deforms by ductile flow without visible structures at the seismic scale (Figure 2a). Fault zones are often poorly imaged on seismic data, but they can be inferred by the fanning geometries of syn-kinematic sedimentary sequences. On a regional scale, continental extension focuses with time and results in the formation of a crustal necking zone where the basement and Moho surfaces converge.

When the crust is less than ~10 km thick, all of it is in the brittle regime. Under these rheological conditions, low angle faults can now cut through the lower crust and may offset the Moho, resulting in highly rotated, rafted crustal fragments that characterize the hyperextended domain (Figure 2b). As detachments become almost horizontal, syn-kinematic sequences change from fanning to subparallel stratal geometries in this domain.

In the absence of magmatic processes, further extension may lead to the exhumation of continental mantle, already serpentinized at depth, to create new real estate beyond the exhumation point (Figure 2c). Although difficult to recognize seismically, the syn-kinematic sequences would downlap towards the proximal exhumation point. The serpentinization front can extend 2-4 km (0.7-1.3 s TWT) below mudline and may cause a faint, discontinuous seismic event. Because of its relatively higher density and small thickness, the serpentinized mantle layer generally coincides with the lowest point in the basement. Typically, there is a 1-1.5 km step-up from exhumed mantle onto normal oceanic crust.

Exhumed mantle can be difficult to distinguish from oceanic crust formed by ultra-slow seafloor spreading (Figure 2d), which also results in a 2-4 km thick crust (Dick *et al.* 2003) and

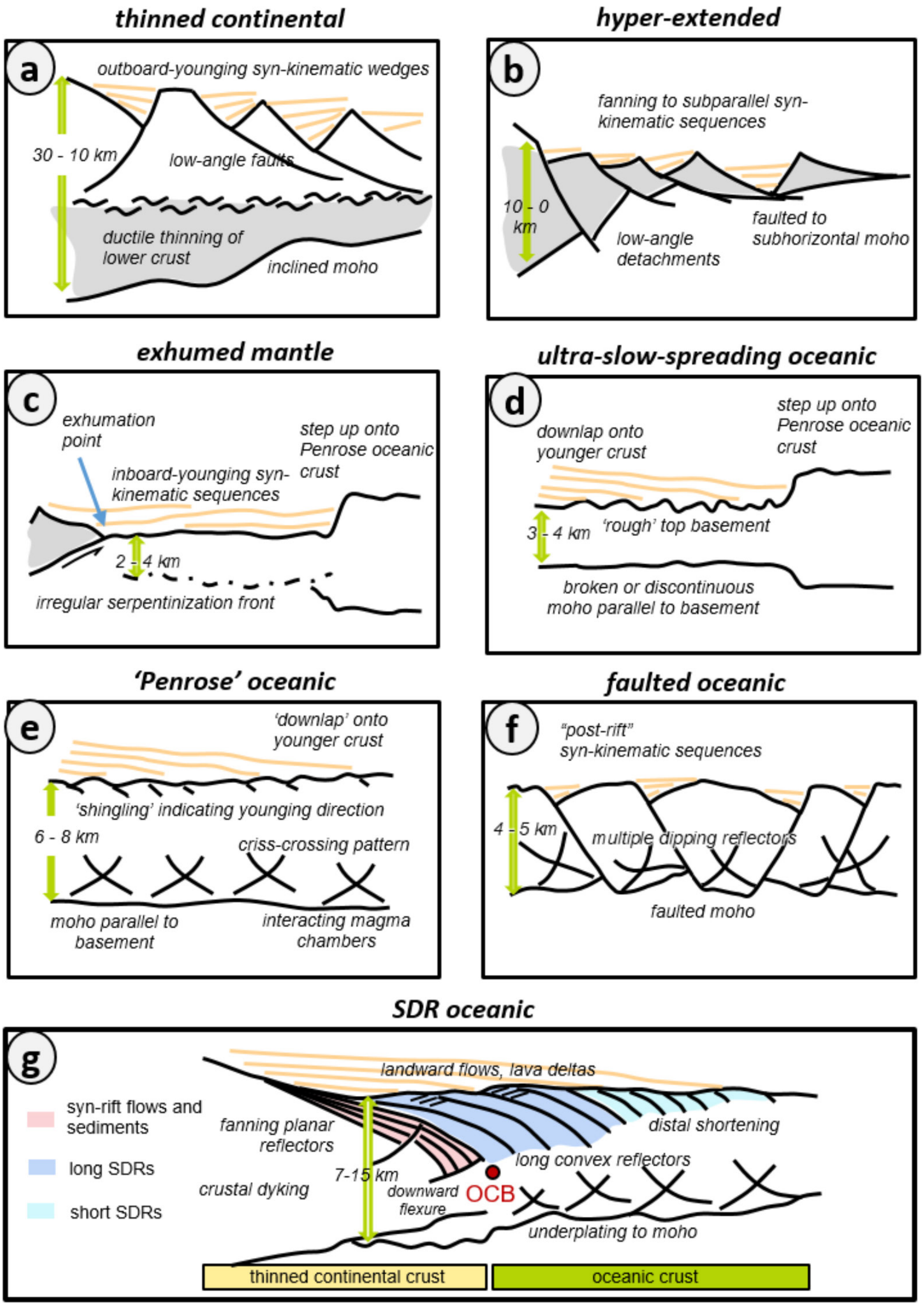

Figure 2. Sketches illustrating our criteria for characterizing and defining crustal types and the Ocean-Continent Boundary (OCB) on the basis of seismic character, crustal thickness, and basement and Moho geometries. Orange lines show common sedimentary patterns and terminations associated with basement deformation (a-c) and younging directions (d-g).

where the deep basement will step up onto Penrose oceanic crust. Thin oceanic crust can be recognized by its rough basement topography, the presence of a Moho, and downlapping sediments above.

Penrose oceanic crust has a uniform thickness in the range of 6–8 km (2–2.5 s TWT) with a well-imaged seismic Moho parallel to the basement (Figure 2e). It is comprised of two layers with distinct seismic facies: Layer 2, a semi-transparent upper zone of sheeted dikes and capped by pillow basalts; and a lower Layer 3 of relatively high amplitude, criss-crossing reflections representing lower crustal gabbros and cumulates. A faint seismic 'shingling' at the basement level will indicate the younging direction of the oceanic basement.

Faulting of oceanic crust can reduce its thickness, create additional deep reflectors, and even display syn-kinematic, post-breakup sedimentary sequences (Figure 2f). Unlike continental crust fragments, this crust is mostly tabular and can extend laterally for hundreds of kilometers.

2.2. Magmatic Seaward Dipping Reflectors

Magmatic Seaward Dipping Reflectors (SDRs) develop in the transition between continental and oceanic crust when active magmatism precedes and accompanies the breakup process. As they originate in subaerial seafloor spreading environments, they are necessarily symmetric, implying crusts having opposite fabric vergences across the spreading center (often termed SDRs and LDRs, Landward Dipping Reflectors). The subaerial settings of SDRs are a consequence of either thick magmatic crust associated with plume activity (e.g., Pelotas Basin and Iceland), or normal crustal thicknesses in which the along-strike paleobathymetry is controlled by regional barriers (e.g., Malvinas Plateau and the proto-Walvis Ridge). Thus, while SDRS are often a product of magma-rich margins, the crust need not be thick nor associated with mantle plumes. Individual SDR packages thin away from the source and, where drilled, consist of subaerial tholeiitic basalts with a relatively simple bulk chemistry.

Seismically-imaged SDRs represent a geometric arrangement of stacked volcanic flows with a consistent concave-downward motif. Reflector geometries represent the chronostratigraphy of superimposed, composite volcanic flows (i.e., timelines) that progressively young in the direction of volcanic source and spreading center migration. Each flow downlaps (which rotates to an apparent onlap) onto earlier SDRs or extended continental crust. We recognize two main types of seaward-dipping geometries among the margin (Figure 2g): An inboard set of diverging reflectors that roughly appear to fan about a common point, indicating listric fault control; this package is similar to the internal SDRs of Geoffroy (2005), Chauvet *et al.* (2021) or the type 1 SDRs of McDermott *et al.* (2018). On the proximal side, these reflectors are planar and can terminate relatively high against the thinned continental margin (e.g., Figure 6). These reflectors, which we map as syn-rift flows, are generally straight and may curve down slightly on the distal or basinward side, where they are overlain by the typical SDRs ("oceanic SDRs" of Geoffroy (2005); type 2 of McDermott *et al.* 2018). The outer set of seaward-dipping reflectors, or magmatic SDRs in this work, are concave down, they become diffuse at mid-crustal levels on the distal end, and exhibit both a vertical and a lateral stacking component.

Despite their morphological similarities, we assign important genetic implications to both types of seaward-dipping reflectors, as discussed in Paton *et al.* (2017), Karner *et al.* (2021) and outlined in Figure 2g. Fanning, fault-controlled packages are underlain by thinned continental crust and represent syn-kinematic sequences of sediments and lava flows emplaced during the crustal rifting stage. The classic SDRs gradually blend with the layer 2 oceanic crust and therefore represent extensive lava flows associated with post-breakup seafloor spreading; the unusual length that gives their seismic character represents subaerial conditions during lava emplacement. In this scenario, they flow away from a subaerial spreading center, initially extend over the preexisting thinned continental crust, and are later flexed down by the load of subsequent flows as the spreading center migrates. Therefore, SDRs represent oceanic new real estate, and the point of origin of the initial flows indicates the approximate location of the ocean-continent boundary, OCB (Figure 2g, Karner *et al.* (2021).

Additional characteristics and morphologies of SDRs record valuable information pertaining the spatial and temporal evolution of the margin. Here we summarize major characteristics that were mapped in Figure 4 and discussed later in this work.

SDR length: SDR length ranges between 2 and 40 km along the margin (McDermott *et al.* 2018, 2019); longer flows (12-20 km) are observed inboard and may maintain a uniform length for several 10s km, and later, transition to flows that are 3-5 times shorter (<~5 km) over a distance of 20 to 60 km. Outboard of this zone, the SDRs appear as short, shingled reflectors in Penrose oceanic crust. In Figure 3, we used the location of rapid shortening rather than a length threshold to discriminate between long and short SDRs, and from short SDRs to Penrose oceanic crust. We postulate that long SDRs represent subaerial lava flows, short SDRs reflect an emergent spreading center and flows in shallow water conditions, and oceanic 'shingles' as flows of pillow lavas from a submerged spreading center.

Lava deltas: When lavas intersect a body of water (lake or ocean), a lava delta is produced by rapid quenching and fragmentation of flows to create a talus of prograding foresets (e.g., Abdelmalak *et al.* 2016). While the Argentina-Uruguay margin provides few and poor lava delta examples, excellent lava deltas associated with a subaerial spreading center are seen in the Namibe basin (Figure 3b), conjugate to the northern part of our study area. The prograde direction of the lava delta, towards the margin, confirms that SDRs are rotated timelines of volcanic flows sourced from a subaerial spreading center. Therefore, the lava delta topsets track paleo-shoreline positions while the relief of the delta front is a proxy for paleo-water depth through time.

Younging direction: As previously mentioned, the lateral stacking of SDR flows reflect the migration of the spreading center with time, where younger flows progressively offlap older flows, thus revealing the younging direction of the oceanic crust (Figure 3). Most of the margin shows the expected progressive younging to the east, consistent with magnetic anomaly chrons (e.g., Lovecchio *et al.* 2020), and along strike to the north, consistent with plate separation about an Euler pole located further to the north. However, we have mapped two areas where these younging trends are complicated, i.e., SDRs younging to the south and

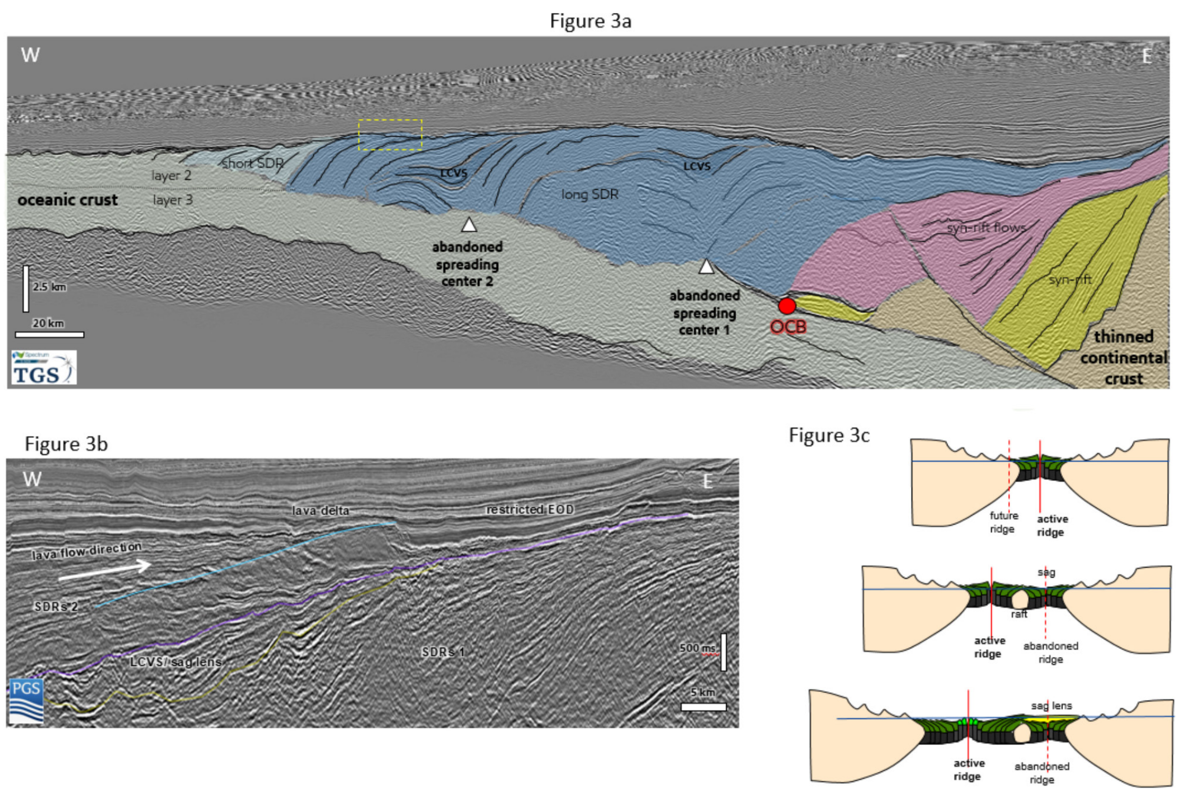

Figure 3. a) Regional seismic profile across the central Orange Basin, South Africa, conjugate to the central and northern segments of the Argentinean margin. The section shows the magmatic SDR geometries associated with tectonic and magmatic processes developed during the initial phases of seafloor spreading. SDRs are basically equivalent to layer 2 of oceanic crust; the different reflector lengths reflect an initially subaerial spreading center that eventually becomes submerged. In this domain, SDRs dip towards the causative spreading center; opposing dips and lens-shaped volcaniclastic bodies indicate spreading centers abandoned after a ridge jump event. The yellow box shows the equivalent location of Figure 3b on a regional line some 100s km to the north. Seismic image courtesy of Spectrum Geo Inc. b) Example of a prominent lava delta associated with SDRs in the northern Namibe basin, Namibia. Talus progradation confirms that flows originate from the distal part of the margin; top sets track the air-water interface with time, while the talus height is a proxy for the paleo-water depth of the restricted depocenter to the east. Seismic image courtesy of PGS. c) Schematic model relating the SDR geometries with ridge jump and abandonment and the development of a sag basin. Along with oceanic crust, ridge migration may incorporate continental allochthons from the conjugate margin; SDR reflections will shorten and eventually merge into a transparent layer once the spreading center becomes submerged.

to the west (LDRs). One of these areas is an ~70 km segment of south-dipping SDRs around the 43° south latitude; the other area, discussed in detail in Section 4, is the southernmost part of the margin, where we document both south- and west-younging reflectors.

Ridge jumps: Flexural rotation of flows that originally dipped away from the emanating spreading center generate a conjugate set of SDR reflections that dip towards the spreading axis (Figure 3c); only one set of reflectors is preserved on the margin, unless a ridge jump captures a piece of the opposite set. Such captured crustal fragments are identified by dipping reflectors that are opposite to those of the SDRs, and they are termed landward-dipping reflectors or LDRs. The area between both sets of reflectors corresponds to the site of the abandoned spreading center, whereas the location of the newly formed spreading center is indicated by a strong angular unconformity or paraconformity (e,g., Thordarson and Höskuldsson 2008; Siler and Karson 2017). Excellent examples of ridge jumps within an SDR domain exist in the margin conjugate to the study area in the Orange, Luderitz, and Namibe basins (Figure 3a). There, the presence of one or more abandoned spreading centers is indicated by LDRs, strong angular unconformities, and/or by small lens-shaped depocenters or laterally confined volcanic successions (LCVS, Norcliffe *et al.* 2018) (Figure 3c). The existence of multiple westward ridge jumps, which incorporate pieces of South American oceanic crust onto Africa, are common during the early phases of seafloor spreading (Buck 2017), and provides an alternative explanation for the asymmetric extent of SDR domains on the South American and SW African margins (e.g., Reuber *et al.* 2019). As we will discuss in the next section, we argue that the southernmost segment of the study area contains the only areas of the margin where the spreading center jumped to the east, leaving behind pieces of African oceanic crust (Simons, *et al.* 2021).

Subsequent faulting and volcanism: After its creation, the oceanic crust (both SDR and Penrose types) can be affected by later tectonic and volcanic processes that may modify its original morphology and topography. In the study area, normal faulting has resulted in the local segmentation and disruption of the SDR reflections, complicating their recognition (Figure 8); in some areas, faulting may be accompanied by early syn-kinematic sequences that are clearly post-breakup, as they occupy accommodation within oceanic crust. It is also important to distinguish that, in contrast with syn-rift (type 1) flows and sediments, faulting is not associated with the typical rotation and curvature of SDR sequences, which is largely flexural. Volcanic activity has taken place after the formation of oceanic crust, mainly south of 43°S latitude, and resulted in the formation of volcanic cones that may locally amalgamate into volcanic complexes. In some cases, paleo base level indicators, such as lava deltas and isolated carbonate buildups, can be observed associated with these volcanic features.

3.1. Margin framework description

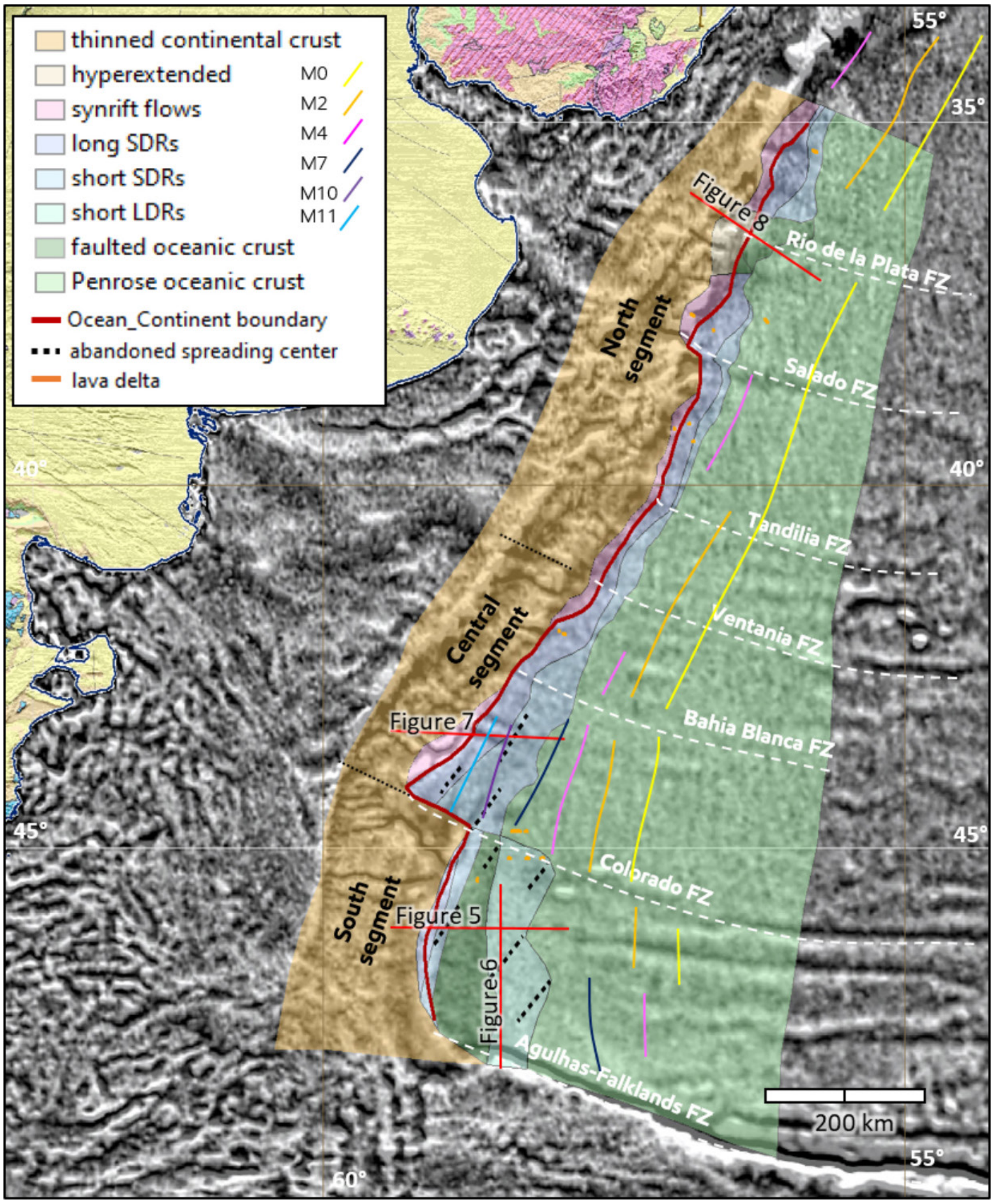

Figure 4. Crustal domains along the Argentina deep-water margin, mapped using the criteria outlined in Figure 2, allowing a precise determination of the continent-ocean boundary. In addition, the location of proposed abandoned spreading centers in the southern segment –see Figure 10a– and possible lava delta features associated with SDRs and early seamounts are also shown. Onshore Surface Geology data licensed by Geologic Data Systems; offshore gravity data from Sandwell *et al.* (2013); magnetic anomalies from Lovecchio *et al.* (2020).

Figure 4 shows the distribution of crustal domains and magmatic features that were mapped using the criteria outlined in the previous section.

At the simplest level, the crustal framework of the margin is characterized by a continuous belt, 50-90 km wide, where syn-rift flows transition at the OCB to long SDRs, short SDRs, and finally Penrose oceanic crust related to the creation of new real estate. The belt is continuous, with lateral steps that continue as oceanic fracture zones. The distance between the OCB and different magnetic anomalies seems to suggest a strong diachroneity, younging from south to north, along the margin. However, as we show later, this is difficult to reconcile with the established breakup ages for southern Argentina (M11;Lovecchio *et al.* 2020) and the Santos Basin (134-132 Ma; Karner *et al.* 2021).

In terms of crustal architecture, we can divide the margin into three main segments, north, central, and south, typified respectively by the seismic sections in Figures 5-8.

South Segment (Figure 5), located between the Agulhas-Falklands and the Colorado fracture zones: The width of SDR oceanic crust outboard of the OCB is ~65 km, with first long flows extending eastward 15-20 km over thinned continental crust. The western half of the belt are comprised of SDRs, a portion of which are highly faulted, whereas the outer half are LDRs, defining an abandoned spreading center between both packages. We have argued previously (Simons *et al.* 2021) that the area is among the earliest depocenters along the entire margin, with restricted conditions favorable for source rock deposition. In this scenario, this is the only place on the margin where seafloor spreading jumped to the east of the LDRs, capturing ~35 km of African oceanic crust. Unlike observations further north along the African margin, we note that the conjugate segment south of the Hope FZ is characterized by a steep hinge zone topography, a relatively narrow SDR zone, and no ridge jumps (e.g., Koopman *et al.* 2014). The onset of the final phase of oceanic crust formation is marked by increased faulting of the LDRs crust, after which Penrose oceanic crust with faint shingling to the east was generated, suggesting a deeper base level during this time (Figure 6).

Central Segment (Figure 7), between Colorado and Ventania fracture zones: Some inboard areas in this section show clear examples of fault-controlled, rectilinear syn-rift flows, while they are missing in other areas. The central segment is characterized by the progressive narrowing of the magmatic domain to the north, from ~150 km north of the Colorado FZ to ~60 km wide approaching the Ventania fracture zone. Unlike the southern segment, all the magmatic units are in the central area are seaward-dipping, progressively younging to the east. In this section the magmatic domain is best developed and the archetypal progression of syn-rift flows to long SDRs, short SDRs, ending in Penrose oceanic crust can be clearly seen. A distinct Moho reflection is visible across the margin, showing that the crust is ~13 km thick over long SDRs, 10-11 km over short SDRs, and 7 km over Penrose oceanic crust. This gradual thinning reflects a decreasing magmatic budget (i.e., dissipating thermal anomaly) with time (Karner *et al.* 2021). These SDRs are conjugate to the outermost set of SDRs in the Orange Basin; the earlier sets were attached to the South African margin via a series of ridge jumps (Figure 3). The paleogeographic evolution of the central segment appears to be diachronous, probably reflecting the progressive deepening of the ocean basin; for example, the transition from short SDRs to Penrose crust (i.e., spreading center becomes submerged) takes place by M7 time in the south and by M4 in the north.

North Segment (Figure 8), north of Ventania FZ to the Porto Alegre FZ: The style and distribution is similar to the Central segment, but this area has a rather constant width of 50-55 km and a more continuous presence of type 1, syn-rift flows. Importantly, the belt of SDRs is interrupted by an area of hyperextension around the Rio de la Plata FZ (~35.5°S), at the intersection with the Punta del Este basin (Figure 4). As mentioned earlier, the hyperextended domain is characterized by low angle faults that rotate crustal fragments and offset the Moho, further thinning the crust and resulting in a deep depocenter at the OCB. Subsequent magmatic activity resulted in the overprinting of the outer portion of the basin with lava flows and the construction of a magmatic outer basin high that constitutes the steep, distal end of the depocenter. No syn-kinematic sequences or interfingering of sediments and flows were observed within the hyperextended depocenter, suggesting that some time elapsed between tectonic/magmatic activity and the onset of clastic sedimentation. In this area the SDR morphology cannot be discerned, either because it has been highly fragmented and rotated, or because this branch of the Salado/Punta del Este rift was still active during the earliest phases of Atlantic spreading, resulting in a short-lived triple junction. The paleogeographic evolution of this margin segment is diachronous, with evidence of deep-water incursion by M4 time in the south and M2 in north.

4. Evolution of the Argentina Basin

Continental breakup is the process by which a lithospheric plate is vertically broken and a new plate boundary is formed. It is also the moment where the localization of intraplate extension (rifting) and related lithospheric thinning ceases, giving way to seafloor spreading and oceanic crust generation. Oceanic crust is formed at spreading centers by the decompressive melting of the underlying asthenosphere to form tholeiitic basalt (McKenzie and Bickle 1988), which is relatively homogeneous in composition and typically 6-8 km thick. However, in regions characterized by elevated upper mantle temperatures, such as might be expected in the vicinity of a plume, an increase of mantle temperature can result in relatively thick melts. In the literature, the term “Penrose” oceanic crust is reserved for “true” oceanic crust; oceanic crust thicker or thinner than 6–8 km is not considered Penrose. We note, however, that the thick oceanic crust of Iceland (elevated mantle temperature), the thin oceanic crust of the Gakkel Ridge or the Australian-Antarctic convergence (ultraslow spreading or reduced mantle temperature, respectively), or Penrose oceanic crust (normal mantle temperature), all represent

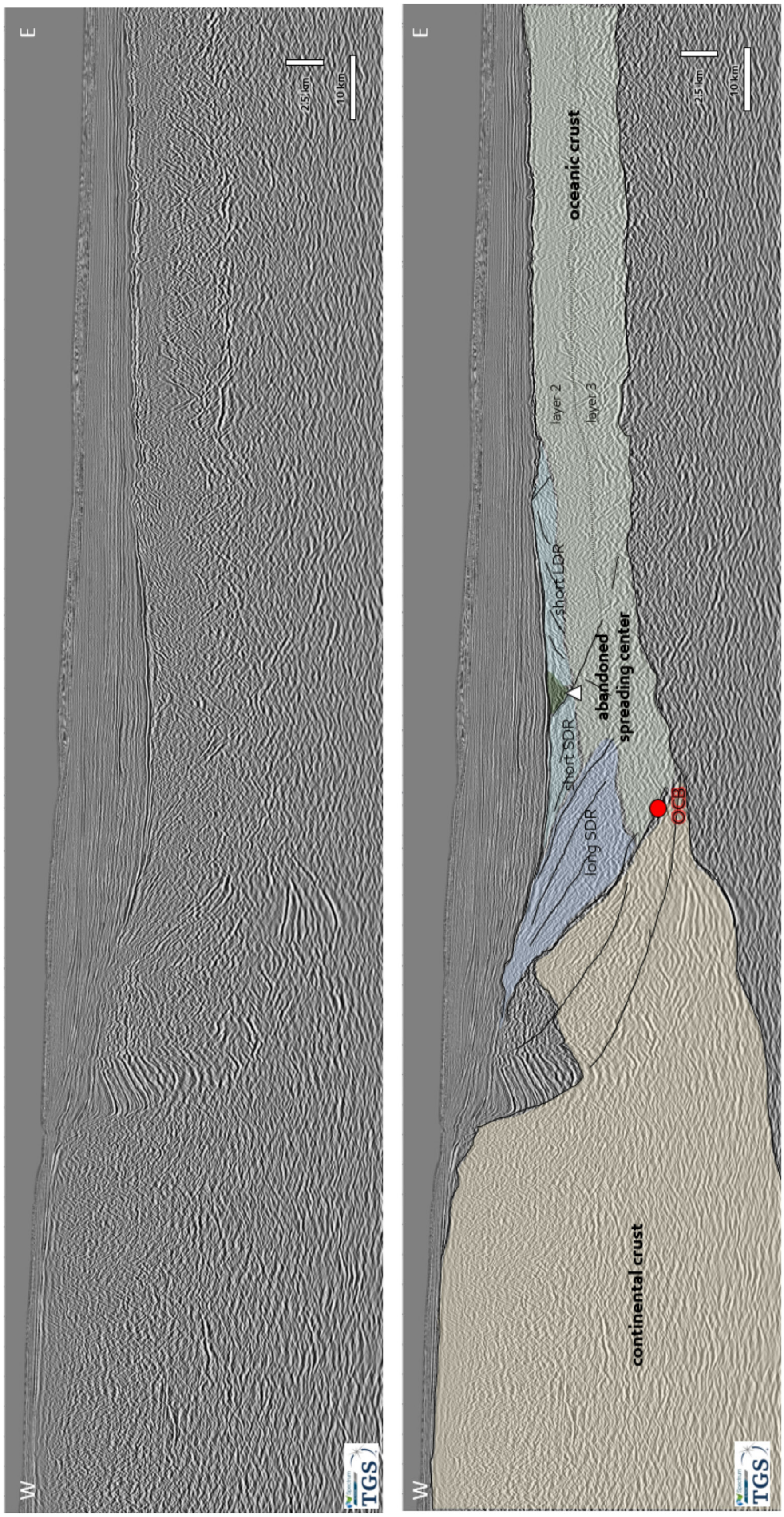

Figure 5. Regional seismic line across a representative area of the southern segment of the margin, showing the transition from tectonic to magmatic processes. After lithospheric breakup, long SDR flows originate from the new spreading center (at the OCB) and initially flow across thinned continental crust; subsequent flows comprising the extrusive part of oceanic crustal layer 2, shorten as the spreading center becomes submerged. As magmatic SDRs dip towards the causative spreading center, the set of west-dipping LDRs help define the location of an abandoned spreading axis in the southern segment. Seismic image courtesy of Spectrum Geo Inc.

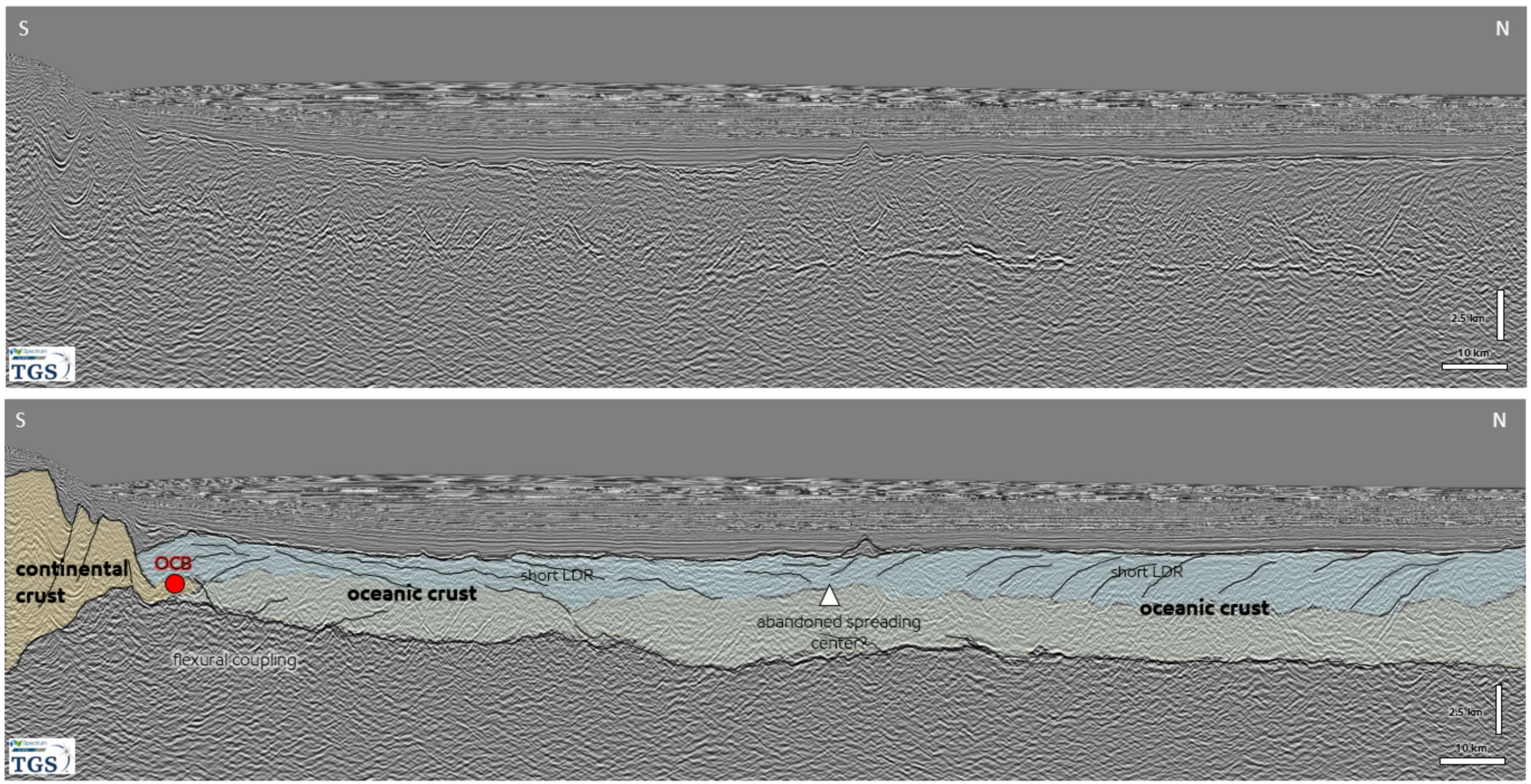

Figure 6. Regional seismic line along the distal part of the southern segment of the margin showing both north- and south-dipping SDRs. As in previous examples, the area where both reflector sets face each other indicates the location of one of several abandoned spreading axis in the southern segment. This is an apparent dip, with the true dip suggesting a NE-SW spreading center orientation. The image also shows the flexural coupling associated with the sharp transition from thinned continental to oceanic crust in the southern corner of the Argentina basin. The coupling is evidenced by the upward flexure of the oceanic basement and Moho interfaces, in addition to the sharp unconformity in the sedimentary section. Seismic image courtesy of Spectrum Geo Inc.

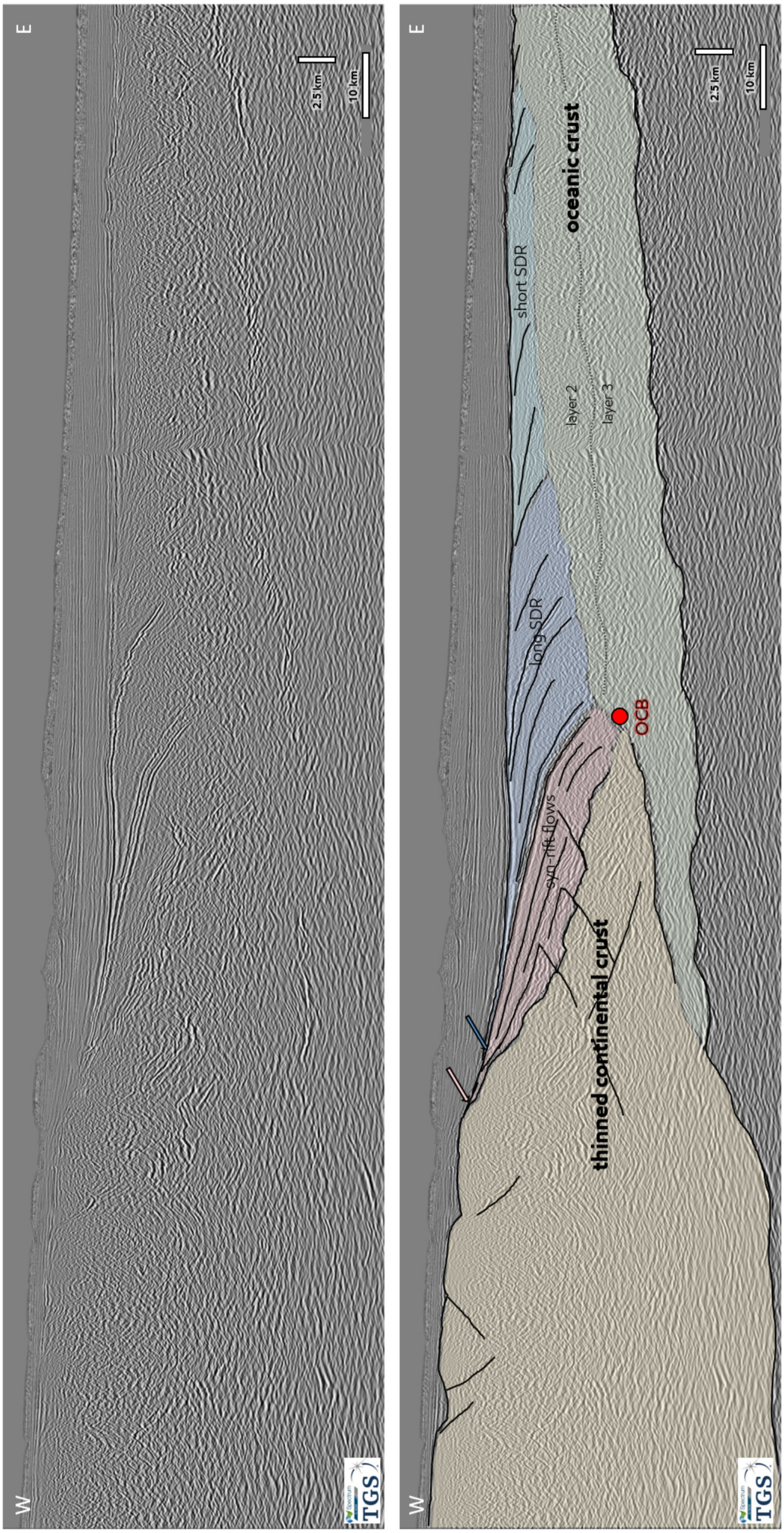

Figure 7. Regional seismic line across a representative area of the central segment of the margin, showing the transition between SDRs and syn-rift flows. Syn-rift volcaniclastic wedges occupy fault-controlled accommodation within the thinned continental crust, while post-breakup SDR geometries are controlled by crustal flexure and spreading center migration. Note that syn-rift flows and SDRs have different distal onlap points along the margin. Seismic image courtesy of Spectrum Geo Inc.

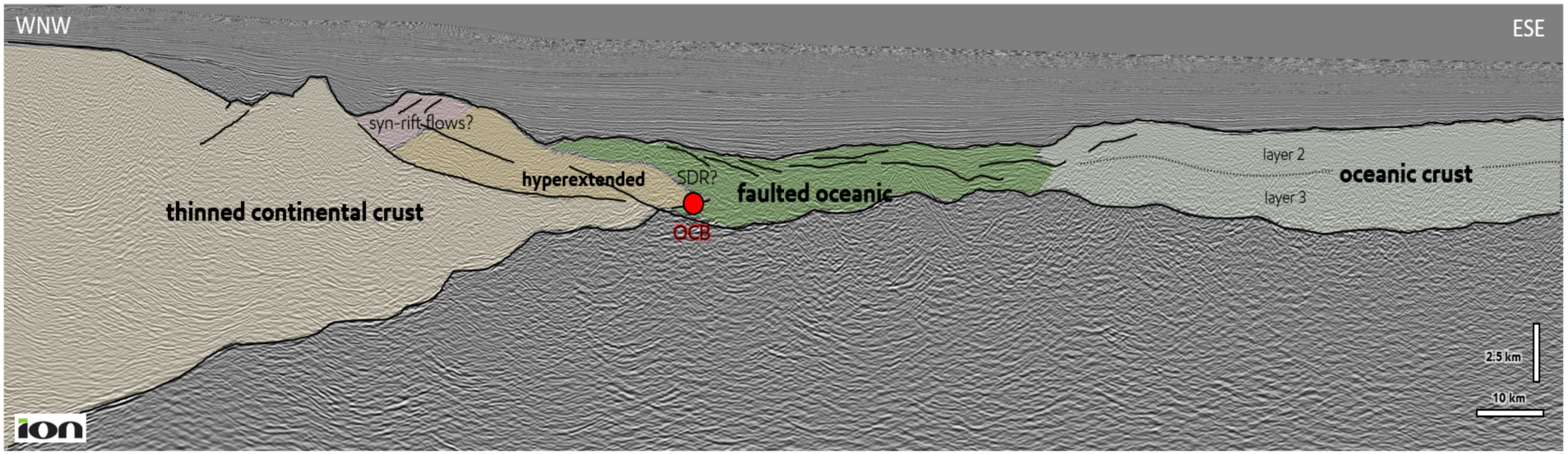

Figure 8. Regional seismic line across an area of the northern segment of the margin in the vicinity of the Rio de la Plata fracture zone where the tectonic deformation continued after breakup. Along most of the northern segment, the crustal domains resemble the central segment. However in this area, continued extension has resulted in hyperextension of the continental crust and faulting of the early oceanic crust. The lack of clear SDR geometries here may be due to possible flooding of this deeper area of the margin, where the crust is thinnest, or to their disruption by faulting. Seismic image courtesy of ION.

the decompressive melting of mantle in response to plate divergence. For this continuum of oceanic crust generation, we consider Penrose oceanic crust to be associated with "normal" asthenosphere temperatures (1333°C), while we term thicker and thinner oceanic crusts as magmatic. In all cases, these variations of oceanic crust consist of a two-layered crustal system dominated by an upper layer of basalts and sheeted dykes and a lower layer of isotropic and cumulate gabbros.

We have concentrated on SDR timing, distribution, and vergence along the southern Argentinian SDRs in order to delineate the temporal and spatial variations of the earliest depocenters along the margin. Understanding the tectonic evolution, subsidence, and age of the opening of the basin may provide insight into early environments of deposition (EODs) that may not be present along other parts of the Argentina/Uruguay margin and conjugate. In general, we recognize two fundamentally different magmatic systems characterizing the Argentina margin: 1) syn-rift, deformed volcanic flows and intercalated sediments infilling syn-rift accommodation, crustal dyke swarms and associated distal flexuring of the thinned continental crust; and 2) post-breakup, essentially undeformed, composite SDR flows that progressively young towards a volcanic source, a spreading center that itself is migrating; as already mentioned, the initial flows of which onlap syn-rift volcanic packages and/or extended continental crust.

Many workers have attempted to reconstruct the South American and African plates across the South Atlantic, thereby prescribing the formation of the South Atlantic oceanic crust as a function of space and time (e.g., Sibuet & Mascle 1978; Rabinowitz & La Brecque 1979; Vink, 1982; Pindell & Dewey 1982). This endeavor has been stymied by the fact that the Cretaceous magnetic quiet zone does not show magnetic reversals. In fact, only the M-series and C-series chrons can be used for plate reconstructions. Rabinowitz and LaBrecque (1979) were the first to define a consistent set of M-series seafloor spreading magnetic anomalies for the South Atlantic margins, thereby establishing the age of continental breakup, Euler pole locations, and the magnitude and timing of spreading center migration. In particular, they defined magnetic Chrons M0-M11 for the West African margin. The quality of the magnetic data, however, was challenged for the South American margin, such that only magnetic Chrons M0-M4 could be reliably recognized (Rabinowitz & LaBrecque 1979). Bird and Hall (2016), using vendor 2D seismic and magnetic profiles, attempted to remap the M-series chrons off the Uruguay and southern Brazilian margins; their mapping repositioned the location of magnetic Chrons M0 and M3 some 160-180 km to the east. Most workers (e.g., Moulin *et al.* 2010; Koopmann *et al.* 2014; Collier *et al.* 2017) generally agree with the Rabinowitz and LaBrecque (1979) picks for M0 and M3 off Uruguay and southern Brazil. Correlatable seafloor spreading magnetic anomalies have not been convincingly recognized in the Pelotas and Santos basins.

Because of this mismatch of magnetic chrons, it was hypothesized that the opening of the South Atlantic occurred diachronously from South to North (e.g. Rabinowitz 1976; Rabinowitz and Labrecque 1979; Austin and Uchupi 1982; Sibuet *et al.* 1984), and described as a successive northward unzipping of rift zones (e.g., Jackson *et al.* 2000). From interpretation of geophysical data, Franke *et al.* (2017) showed that the margin structure, and especially the seaward-dipping reflector formations that characterize the Argentine margin,

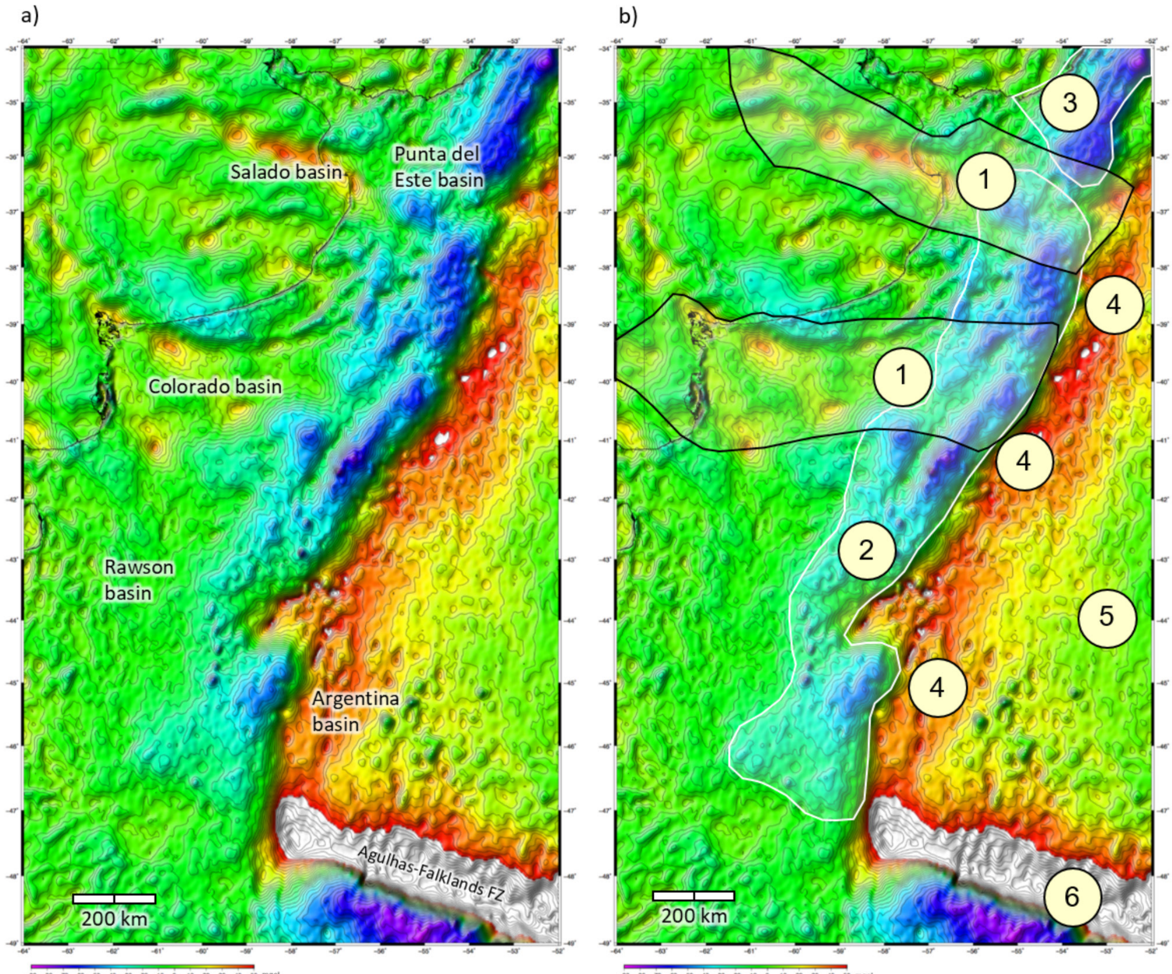

Figure 9. a) Filtered Bouguer gravity anomaly map of the Argentine margin. The Bouguer gravity anomaly was calculated from the Global Free-air gravity (v30; Sandwell *et al.*, 2013) and the GEBCO (2020) bathymetry and topography grids. A topographic density of 2800 kg/m2 and upward continuation distance of 2.5 km was assumed. The resulting filtered Bouguer gravity anomaly was obtained using a high-pass (wavelengths less than 600 km) Gaussian filter. b) Superposition of the Argentinian basin systems on the filtered Bouguer gravity anomaly. The sedimentary basins show an interesting relationship with the filtered gravity. The well-known basins that are generally perpendicular to the margin (Salado, Colorado, Rawson basins) are characterized by central positive gravity anomalies. This paradoxical relationship is a consequence of the flexural interference of low flexural rigidities induced by significant lithospheric extension and increased rigidities associated with the post-rift cooling of the lithosphere and sediment loading. The positive gravity anomaly reflects a period of basin starvation following extension; the larger the gravity anomaly amplitude, the larger the difference in time between extension and sediment deposition. We predict an early-mid Jurassic rift age of the Salado, Colorado, and San Jorge basins, in marked contrast to the broad distribution of small, Late Jurassic-Early Cretaceous rift basins across the continental margin. Numbers refer to particular gravity anomalies: 1) positive central anomalies of the Salado and Colorado basins; 2) zone of broad distribution of late Jurassic-early Cretaceous rift basins across the continental shelf; 3) shallow basement of the Polonio High; 4) SDRs; 5) Penrose oceanic crust; 6) flexural coupling of continental-oceanic crust.

varied significantly in architecture, extent and thickness along strike of the margin. Franke *et al.* (2017) and other workers have misinterpreted the SDRs as part of the syn-rift deformation of the continental crust rather than early post-breakup oceanic crust (e.g., Karner *et al.* 2021). It is possible, therefore, that the "missing" magnetic chrons are represented by these SDR constructs along the margin and whose convoluted magnetic signal maybe difficult to recognize as standard M-series chrons.

Lovecchio *et al.* (2020) has helped remedy this "missing chron" problem for the Argentine margin when they recognized that the southernmost Rawson/Valdés and Outeniqua basins were characterized by Valanginian breakup, implying that the first magnetic chron on this part of the margin should be M11. This is in excellent agreement with detailed, high quality, marine magnetic data acquired off the southwestern margin of South Africa and interpreted by Hall *et al.* (2018). In particular, they recognized a pattern of well-defined, NW-SE striking linear magnetic anomalies interpreted to be M-series seafloor spreading anomalies M11 to M9 (late Valanginian/early Hauterivian). Further, and perhaps just as significantly, Karner *et al.* (2021) have dated the breakup age of the Santos Basin using well data as early Hauterivian-late Valanginian (134-132 Ma; Ogg 2020). The oft-quoted late Aptian breakup age for the Santos Basin (e.g., Mohriak *et al.* 1995; Franke *et al.* 2017; Lentini *et al.* 2010; Scotchman *et al.* 2010; Unternehr *et al.* 2010; Blaich *et al.* 2011; Zalán *et al.* 2011) is, in fact, the transition from ultraslow seafloor spreading to post-salt, Penrose oceanic crust (Karner *et al.* 2021). These Early Cretaceous chron ages, coupled with the drilling ages for breakup in the Santos Basin, question the viability of a diachronous opening, or south-north unzipping, of the southern South Atlantic. An alternative explanation for "missing chrons" is that the magnetic chrons should also be part of the SDR sequences; their magnetic signature is likely complicated by the stacking of magmatic flows and thus difficult to recognize as correlatable seafloor spreading magnetic anomalies. A northerly Euler rotation pole for this early opening would have resulted in significantly more plate separation for the southernmost South Atlantic compared to separation between the Santos and southern Kwanza margins.

To highlight regional structural trends, we have generated a filtered Bouguer gravity map of the Argentine margin (Figure 9a). Using the Global Free-air gravity grid (v30; Sandwell *et al.* 2013), we calculated the gravity effect of the bathymetry and topography (GEBCO, 2020) assuming a topographic density of 2800 kg/m2 and upward continuation distance of 2.5 km. Subtracting the calculated topography gravity effect from the Free-air gravity results in a Bouguer gravity anomaly, which we then filtered with a high-pass, 600 km Gaussian filter (Figure 9a). The resulting negative filtered Bouguer gravity anomaly contrast the broad distribution of minor Late Jurassic-Early Cretaceous sedimentary basins across the shelf from the regional positive anomalies associated with relatively thin oceanic crust. A local but extreme positive-negative anomaly characterizes the flexural coupling across the Falkland Plateau escarpment as hypothesized by Lorenzo and Wessel (1997). Other recognizable tectonic features, such as the continental necking zone, the extended crust related to the Salado and Colorado basins, and the abrupt transition from thinned continental crust to SDR and Penrose oceanic crust have been located on Figure 9b. The association of the negative gravity anomalies with minor but broadly distributed rift basins across the shelf has been verified with the available seismic reflection data. A significant erosional unconformity separates all of these rift basins from the overlying post-rift stratigraphy. There seems to be little relationship between the amplitude of the post-rift subsidence to either the thickness of the syn-rift stratigraphy or the location of the rift basins.

In contrast, the major east-west basins of the Argentine margin, the Salado, Colorado, and San Jorge basins tend to be associated with positive gravity anomalies, especially along their depocenter axes (Figure 9b). This situation is counterintuitive in as much that sedimentary basins are generally characterized by negative gravity anomalies, either free-air or Bouguer. As demonstrated by Karner *et al.* (2005), however, positive gravity anomalies over extensional basins result from the flexural interplay between the reduction of lithospheric flexural strength by extension compared with the increase of flexural strength during post-rift cooling of the lithosphere. Extension engenders both a syn-rift subsidence and a concomitant rebound of the rifted lithosphere. The subsequent cooling of the rifted lithosphere generates both post-rift subsidence, and an increase in flexural strength with time. Sediment loading will amplify the amplitude of the post-rift subsidence. The distribution and amplitude of the post-rift subsidence is a function of the changing post-rift flexural rigidity. In particular, if there is a delay in post-rift sedimentation, that is, a period of sediment starvation following extension, the gravity anomaly becomes progressively more positive as the offset between rift cessation and sediment deposition increases. In addition, the period of sediment starvation necessarily implies the development of paleo-water depths, which in turn, may be conducive to source rock deposition. If, on the other hand, there is continuous sedimentation during and after rifting, the gravity anomaly is negative.

The so-called syn-rift stratigraphy of the Salado, Colorado, and San Jorge basins is characterized by a near-absence of unambiguous syn-rift packages. Where divergence and rotation of seismic reflectors indicative of differential subsidence and block rotation can be recognized, the mapped thickness of the syn-rift stratigraphy is minor, certainly compared with the distribution and thickness of the overlying post-rift stratigraphy (e.g., Autin *et al.* 2013; Loegering *et al.* 2013; DeVito and Kearns 2022). Loegering *et al.* (2013) mapped a break-up unconformity across the Colorado Basin extrapolated from the adjacent continental margin to determine rift timing. They estimate a margin break-up age as early Barremian. Nevertheless, much of the syn-rift stratigraphy is characterized by bi-directional onlap onto the underlying stratigraphy and/or basement (Loegering *et al.* 2013; DeVito and Kearns 2022). As such, this stratigraphy is necessarily post-kinematic and likely represents post-rift infill of syn-rift accommodation. This situation implies that during extension, the rift basins were basically sediment starved and characterized by significant paleo-water depths. Loegering *et al.* (2013) suggested a rift onset age of at least Kimmeridigian. The positive gravity anomaly that characterizes the Colorado Basin is completely consistent with the predicted rift timing onset, break-up age, paleo-water depth development, and intervals of sediment starvation based on data presented by Loegering *et al.* (2013) and Autin *et al.* (2013). We would further add that extension may have been significantly older than Kimmeridigian, and was likely a discrete event rather than the protracted event spanning Kimmeridgian to early Barremian suggested by Autin *et al.* (2013) and Loegering *et al.* (2013). By analogy, we predict the same flexural, subsidence and paleo-geography behavior for the Salado and San Jorge basins.

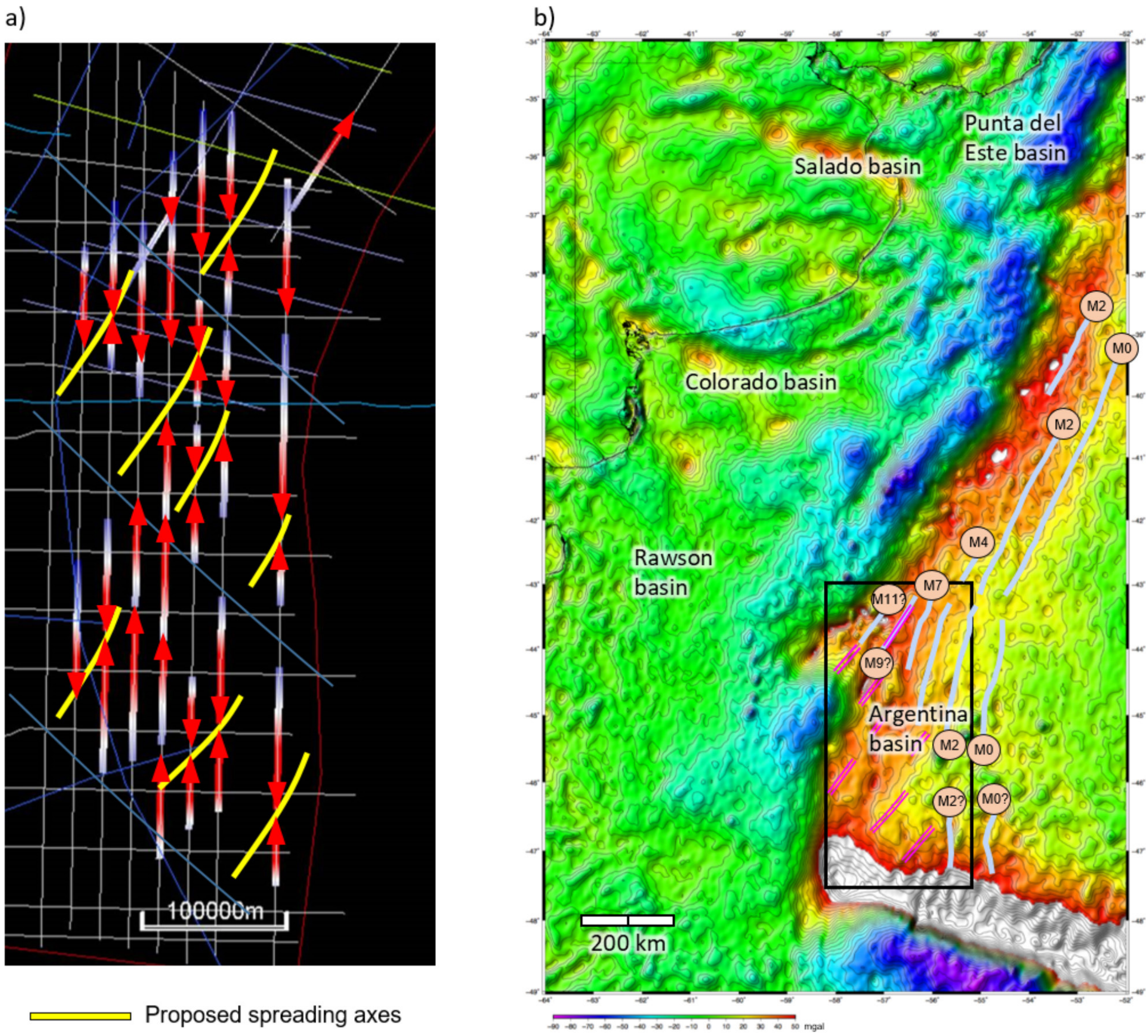

Figure 10. a) Vergence (i.e., dipping directions) of SDR sequences in the southern segment of the margin. For simplicity, only north and south lines are shown; the east and west dipping components can be extracted from the SDR/LDR domains in Figure 4. Facing directions have been used to delineate potential abandoned spreading axes, which are approximately parallel to the earliest magnetic anomalies reported in the area (Chron M7), but oblique to later anomalies. b) Superposition of inferred short spreading centers and implied ages. We assume that the distribution of spreading centers, as defined by opposing SDR vergences, are basically synchronous (Chrons M9-M11), representing unstable and disorganized spreading in the earliest stages of Southern Atlantic breakup. Seafloor spreading became stable following Chron M4.

An interesting anomaly is given by the extreme >50 mgal anomaly that hugs the location of the Agulhas Fracture Zone (Figure 9b). Rather than representing extremely thin crust or zones of mantle exhumation, it actually represents the flexural coupling between the relatively thick continental crust of the Malvinas Plateau and the oceanic crust directly juxtaposed against it. Thermal subsidence of the oceanic crust is retarded in the vicinity of the juxtaposition and is flexed up while the adjacent continental crust is forced to subside. The result is an intense positive-negative gravity anomaly couple across the fracture zone (Figure 9b). Seismic reflection data clearly shows this flexural coupling process and the progressive uplift of the oceanic basement and Moho as it approaches the Agulhas Fracture Zone (Figure 6).

In the southwest corner of the Argentine margin, oceanic crustal vergences are anything but simple, with north-south and east-west vergence pairs mapping out a complicated pattern that can be explained by early seafloor generation with NE-SW oriented spreading ridges (Figure 10a). Eight broadly distributed, abandoned spreading ridges have been tentatively mapped, and are superimposed on a filtered Bouguer gravity map (Figure 10a). The gravity anomaly trends (Figure 9b) clearly show the change from the NE-SW disorganized spreading centers associated with Chrons M11-M7 to the broad, organized spreading centers established during Chrons M4-M0 (and younger). We surmise that the ridges are short lived (1-2 m.y.) and were active concurrently. We suggest that the present-day spreading center configuration of Iceland (Thordarson and Höskuldsson 2008) is a useful analogue to explain this early development of oceanic crust between Argentina and South Africa. For Iceland, the plate boundary (spreading centers) consists of two types: 1) in the south, two concurrent spreading centers taking up the divergence; and 2) in the north, a ridge jump from the west to the east and the formation of a single, active plate boundary (Siler and Karson 2017). The NW-SE spreading directions of this southwest corner are consistent with plate reconstructions and magnetic chron ages for southern Argentina and South Africa (e.g., Hall *et al.* 2018). It is interesting to note that the N125°E to N80°E change in spreading direction in the Santos and Campos basins (Johnson *et al.* 2012) occurs at ca. Chron M4 time. It is thus possible that the entire pre-M4 spreading/extension direction along the southern South American margin had the same orientation as the disorganized spreading centers we mapped in the Argentina Basin.

5. Conclusions

We have revisited the crustal framework of the deep-water Argentine margin by detailed characterization and mapping of crustal domains adjacent to the continent-ocean boundary, which is given the ineffective label of "transitional crust" in the literature. We were able to determine regions dominated by tectonic or magmatic processes, or where they coexist. It was particularly important to distinguish between syn-rift volcaniclastic sequences, filling fault-controlled accommodation, from post-breakup SDR oceanic crust that originated from a spreading center. Variations of SDR morphology have been mapped and related to base-level changes during the evolution of the margin.

The aforementioned distribution of crustal units applies to most of the margin, except in the southernmost area, where the earliest phases of seafloor spreading are more clearly expressed. In this southern segment, we have verified the existence of both seaward- and landward-dipping magmatic sequences, in addition to a complex array of north and south-verging reflectors. We have integrated these observations into a series of spreading centers associated with the earliest NW-SE plate separation in the area. The orientation of these abandoned axes is consistent not only with filtered Bouguer gravity patterns, but also with the earliest (M7 and earlier) magnetic chrons on the Argentine and South African margins.

Finally, we note that the breakup ages implied by the M11-M9 magnetic chrons (late Valanginian-early Hauterivian) in the southern portion of the Argentine margin are similar in age to the northerly Santos Basin breakup age as determined from well data. Magnetic chrons of similar ages appear to be missing between these two regions, which may result from the superposition and interference of magnetic reversal signatures in slow spreading segments of the margin. Rather than supporting a diachronous, northward unzipping breakup model, we suggest that this distribution of ages is consistent with synchronous breakup of the entire southern South Atlantic about a northerly Euler pole.

ACKNOWLEDGEMENTS

We want to thank Spectrum Geo Inc., PGS and Ion/GXT for granting permissions to publish the licensed seismic data, to our management for their support to present this work, and to Chris Johnson and other colleagues that helped us develop interpretation concepts and models. We thank the Conference organizers and reviewers for their collaboration and help.

REFERENCES

Abdelmalak, M. M., Planke S., Faleide J. I., Jerram D. A., Zastrozhnov D., Eide S. and Myklebust R., 2016. The development of volcanic sequences at rifted margins: New insights from the structure and morphology of the Vøring Escarpment, mid-Norwegian Margin, J. Geophys. Res. Solid Earth, 121, 5212–5236, doi:10.1002/2015JB012788

Austin, J.A., and Uchupi E., 1982. Continental-oceanic crustal transition off Southwest Africa. American Association of Petroleum Geologists Bulletin 66, 1328–1347.

Autin, J., Scheck-Wenderoth M., Loegering M.J., Anka Z., Vallejo E., Rodriguez J.F., Dominguez F., Marchal D., Reichert C., di Primio R., and Götze H.-J., 2013. Colorado Basin 3D structure and evolution, Argentine passive margin. Tectonophysics, 604, 264-279.

Bird, D.F., and Hall S.A., 2016. Early seafloor spreading in the South Atlantic: new evidence for m-series magnetochrons north of the Rio Grande fracture zone. Geophys. Jour. Int., 206, 835-844.

Blaich, O. A., Faleide J. I., and Tsikalas F., 2011, Crustal breakup and continent-ocean transition at South Atlantic conjugate margins: Journal of Geophysical Research, v. 116, p. B01402.

Buck, W.R., 2017. The role of magmatic loads and rift jumps in generating seaward dipping reflectors on volcanic rifted margins. Earth Planet. Sci. Lett.466, 62–69. https://doi .org /10 .1016 /j .epsl .2017.02 .041.

Chauvet, F., Sapin F., Geoffroy L., Ringenbach J.C., and Ferry J.N., 2021. Conjugate volcanic passive margins in the austral segment of the South Atlantic – Architecture and development. Earth Sci. Rev., v212, p.103461; doi: 10.1016/j.earscirev.2020.103461

Collier, J.S., McDermott C., Warner G., Gyori N., Schnabel M., McDermott K., and Horn B.W., 2017. New constraints on the age and style of continental breakup in the South Atlantic from magnetic anomaly data. Earth and Planetary Science Letters, Volume 477, 1, 27-40.

DeVito, S., and Kearns H., 2022. Overview of the exploration potential of offshore Argentina – insight from new seismic interpretations. Petroleum Geoscience, 28, 1-22. https://doi.org/10.1144/petgeo2020-132

Dick, H. J. B., Lin J., and Schouten H., 2003. An ultraslow spreading class of ocean ridge. Nature, v. 426, p. 405-412.

Figueredo, P.H., Sullivan M.A., Johnson C.A., Karner G.D., and Sutton S.T., 2017. Tectonic History and Structural Evolution of the East Africa Margin. Conf. Proc., Third EAGE Eastern Africa Petroleum Geoscience Forum, Nov 2017, v. 2017, p.1–4, doi: https://doi.org/10.3997/2214-4609.201702397

Franke, D., Neben S., Ladage S., Schreckenberger B., and Hinz K., 2017. Margin segmentation and volcano-tectonic architecture along the volcanic margin off Argentina/ Uruguay, South Atlantic: Marine Geology, v. 244, p. 46–67

GEBCO Compilation Group, 2020. GEBCO 2020 Grid (doi:10.5285/a29c5465-b138-234d-e053-6c86abc040b9)

Geoffroy, L., 2005. Volcanic passive margins: Comptes Rendus Geoscience, v. 337, p. 1395–1408, doi:10.1016/ j.crte.2005.10.006.

Goudarzi, G.H., 1977. Geologic map of South America, Miscellaneous Field Studies Map 868-A, USGS, https://doi.org/10.3133/mf868A

Hall, S.A., Bird D.E., McLean D.J., Towle P.J., Grant J.V., and Danque H.A., 2018. New constraints on the age of the opening of the South Atlantic basin. Mar. Petrol. Geol. 95, 50-66.

Jackson, M.P.A., Cramez C., and Fonck J-M, 2000. Role of subaerial volcanic rocks and mantle plumes in Creation of south Atlantic margins: implications for salt tectonics and source rocks. Mar. Petrol. Geol. 17, 477-498.

Johnson, C.A., Karner G.D., Kneller E.A., and Kraus J.U., 2012. High resolution plate reconstructions of the South and Equatorial Atlantic. Deep-Water Continental Margins, Geological Society, London, 1-2 October, 2012.

Karner, G.D., Studinger M., and Bell R.E., 2005. Gravity anomalies of sedimentary basins and their mechanical implications: Application to the Ross Sea basins, West Antarctica. Earth Planet. Sci. Letts., 235, 577-596.

Karner, G. D., Johnson C., Shoffner J., Lawson M., Sullivan M., Sitgreaves J., McHarge J., Steward J., and P. Figueredo, 2021, Tectono-magmatic development of the Santos and Campos basins, offshore Brazil. In Marcio R. Mello, Pinar O. Yilmaz, and Barry J. Katz (eds). The supergiant Lower Cretaceous pre-salt petroleum systems of the Santos Basin, Brazil: AAPG Memoir 124, 215–256.

Koopmann, H., Franke, D., Schreckenberger, B., Schulz, H., Hartwig, A., Stollhofen, H., and di Primio, R., 2014. Segmentation and volcano-tectonic characteristics along the SW African continental margin, South Atlantic, as derived from multichannel seismic and potential field data. Marine and Petroleum Geology 50, 22–39. https://doi.org/10. 1016/j.marpetgeo.2013.10.016.

Kress, P., Catuneanu O., Gerster R., and Bolatti N., 2021. Tectonic and stratigraphic evolution of the Cretaceous Western South Atlantic. Marine and Petrol. Geol., https://doi.org/10.1016/j.marpetgeo.2021.105197

Lentini, M.R., Fraser, S.I., and Davies, R., 2010. Geodynamics of the central South Atlantic conjugate margins: implications for hydrocarbon potential. Petrol. Geosc., 16, 217-229, https://doi.org/10.1144/1354-079309-909.

Lorenzo, J.P., and Wessel P., 1997. Flexure across a continent-ocean fracture zone: the northern Falkland/Malvinas Plateau, South Atlantic. Geo-Marine Letters, 17, 110-118.

Loegering, M.J., Anka Z., Autin J., di Primio R., Marchal D., Rodriguez J.F., Franke D., and Vallejo E., 2013. Tectonic evolution of the Colorado Basin, offshore Argentina, inferred from seismo-stratigraphy and depositional rates analysis. Tectonophysics, 604, 245-263. http://dx.doi.org/10.1016/j.tecto.2013.02.008.

Lovecchio, J.P., Rohais, S., Joseph, P., Bolatti, N.D., and Ramos, V.A., 2020. Mesozoic rifting evolution of SW Gondwana: A poly-phased, subduction related, extensional history responsible for basin formation along the Argentinean Atlantic margin, Earth-Science Reviews, v. 203, p. 1-27

McKenzie, D., and Bickle M. J., 1988. The volume and composition of melt generated by extension of the lithosphere. Journal of Petrology, v. 29, p. 625–679.

McDermott, C., Lonergan, L., Collier, J. S., McDermott, K. G., and Bellingham, P., 2018. Characterization of seaward-dipping reflectors along the South American Atlantic margin and implications for continental breakup. Tectonics, 37, 3303–3327. https://doi.org/10.1029/2017TC004923

McDermott, C., J.S. Collier, L. Lonergan, J. Fruehn & P. Bellingham, 2019. Seismic velocity structure of seaward-dipping reflectors on the South American continental margin. Earth Planet Sci. Letts., 521, 14-24.

Mohriak, W. U., J. H. L. Rabelo, R. D. Matos, M. C. Barros, 1995. Deep seismic reflection profiling of sedimentary basins offshore Brazil: Geological objectives and preliminary results in the Sergipe Basin. Journal of Geodynamics, v. 20, p. 515–539

Moulin, M., D. Aslanian, and P., Unternehr, 2010. A new starting point for the South and Equatorial Atlantic Ocean. Earth-Science Reviews, v. 98, p. 1–37.

Norcliffe, J.R., D.A. Paton, E.J. Mortimer, A.M. McCaig, H. Nicholls, K. Rodriguez, N. Hodgson, D. Van der Spuy, 2018. Laterally Confined Volcanic Successions (LCVS); recording rift-jumps during the formation of magma-rich margins. Earth and Planetary Science Letters, 504. pp. 53-63. ISSN 0012-821X. https://doi.org/10.1016/j.epsl.2018.09.033

Ogg, J.G., 2020. Geomagnetic Polarity Time Scale, Geologic Time Scale 2020, Volume 1, Chap. 5, 159-192.

Paton, D.A., J. Pindell, K. McDermott, P. Bellingham, and B. Horn. 2017. Evolution of seaward-dipping reflectors at the onset of oceanic crust formation at volcanic passive margins: Insights from the South Atlantic. Geology, 45, 439-442.

Pindell, J., and Dewey J. F., 1982. Permo-Triassic reconstruction of western Pangea and the evolution of the Gulf of Mexico/Caribbean region: Tectonics, v. 1, p. 179–211.

Rabinowitz, P.D., 1976. A geophysical study of the continental margin of the Southern Africa. Geological Society of America Bulletin 87, 1643–1653.

Rabinowitz, P. D., and LaBrecque J., 1979. The Mesozoic South Atlantic Ocean and evolution of its continental margins: Journal of Geophysical Research, v. 84, 5973–6002.

Reuber, K., Mann P., and Pindell J., 2019. Hotspot origin for asymmetrical conjugate volcanic margins of the austral South Atlantic Ocean as imaged on deeply penetrating seismic reflection lines interpretation, v7 (4): SH71–SH97. https://doi.org/10.1190/INT-2018-0256.1

Sandwell, D.T., Garcia E., Soofi K., Wessel P., and Smith W.H.F., 2013, Towards 1 mGal global marine gravity from CryoSat-2, Envisat, and Jason-1. The Leading Edge, v. 32, no. 8, p. 892–899.

Scotchman, I. C., Gilchrist G., Kusznir N. J., Roberts A. M., and R. Fletcher, 2010, The breakup of the South Atlantic Ocean: Formation of failed spreading axes and blocks of thinned continental crust in the Santos Basin, Brazil, and its consequences for petroleum system development, in B. A. Vining and S. C. Pickering, eds., From mature basins to new frontiers—Proceedings of the 7th petroleum geology conference. Geological Society of London, Petroleum Geology Conference Series, v. 7, 855–866.

Sibuet, J.-C., and Mascle J., 1978, Plate kinematic implications of the Atlantic Equatorial fracture zone trends. Journal of Geophysical Research, v. 83, p. 3401–3421.

Sibuet, J.C., Hay, W.W., Prunier, A., Montadert, L., Hinz, K. and Fritsch, J., 1984. Early evolution of the South Atlantic Ocean: role of the rifting episode. Initial Reports of DSDP, 75: 469-481.

Siler, D.L. and Karson J.A., 2017. Along-Axis Structure and Crustal Construction Processes of Spreading Segments in Iceland: Implications for Magmatic Rifts. Tectonics, doi: 10.1002/2017TC004629.

Simons, K., Figueredo P., Mapes R., and Musso L., 2021. Timing of the Opening of the South Atlantic. GSL Petroleum Geol. of the Southern South Atlantic, Conf. Abst.

Thordarson, T., and Höskuldsson Á., 2008. Postglacial volcanism in Iceland. JÖKULL No. 58, 197-228

Unternehr, P., Peron-Pinvidic G., Manatschal G., and Sutra E., 2010. Hyper-extended crust in the South Atlantic: In search of a model. Petroleum Geosciences, v. 16, p. 207–215.

Vink, G. E., 1982, Continental rifting and the implications for plate tectonic reconstructions. Journal of Geophysical Research, v. 87, p. 10677–10688.

Zalán, P.V., Severino M.C.G., Rigoti C.A., Magnavita L.P., Oliveira J.A.B., and Vianna A.R., 2011. An entirely new 3D view of the crustal and mantle structure of a South Atlantic passive margin–Santos, Campos and Espírito Santo basins, Brazil. Search and Discovery Article #30177, accessed December 15, 2020, http://www.searchanddiscovery.com/ pdfz/documents/2011/30177zalan/ndx_zalan.pdf.html